THE JOURNAL OF PHYSICAL CHEMISTRY A
A JOURNAL OF THE AMERICAN CHEMICAL SOCIETY

pubs.acs.org/JPCA

Article

Extending the Applicability of the Semi-experimental Approach by Means of "Template Molecule" and "Linear Regression" Models on Top of DFT Computations

Alessio Melli,[§] Francesca Tonolo,[§] Vincenzo Barone,[*] and Cristina Puzzarini[*]

Cite This: *J. Phys. Chem. A* 2021, 125, 9904−9916

Read Online

ACCESS | Metrics & More | Article Recommendations | Supporting Information

ABSTRACT: The accurate determination of equilibrium structures for isolated molecules plays a central role in the evaluation and interpretation of stereoelectronic, thermodynamic, and spectroscopic properties. For small semi-rigid systems, state-of-the-art quantum-chemical computations can rival the most sophisticated experimental results. For larger molecules, cheaper yet accurate approaches need to be defined. The double-hybrid rev-DSD-PBEP86 functional already delivers remarkable results that can be further improved by means of a "Lego brick" model. This is based on the idea that a molecular system can be seen as formed by different fragments (the "Lego bricks"), whose accurate semi-experimental (SE) equilibrium geometries are available. The template molecule (TM) approach can be used to account for the modifications occurring when going from the isolated fragment to the molecular system under investigation, with the linear regression (LR) model employed to correct the linkage between the different fragments. The resulting TM-SE_LR approach has been tested with respect to available SE equilibrium structures and rotational constants. Indeed, the latter parameters straightforwardly depend on the equilibrium geometry of the system under consideration. The main outcome of our study is the reliability, robustness, and accuracy of this novel approach. The molecular systems considered for benchmarking the TM-SE_LR scheme are those formally issued from addition/elimination reactions of nucleophilic unsaturated radicals (e.g., CN, C_2H, and phenyl) to alkenes, imines, and aldehydes, whose rotational spectra have been investigated, but accurate structural determinations are not yet available.

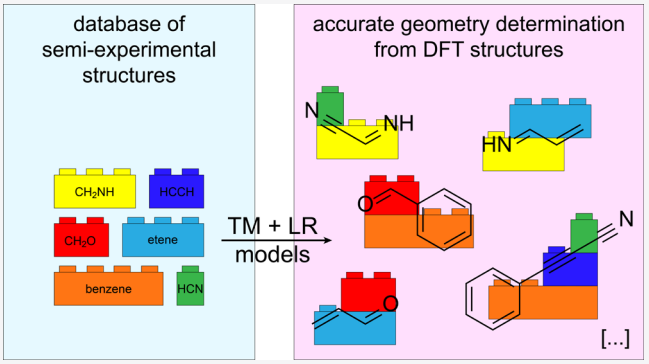

INTRODUCTION

The accurate determination of molecular structures is one of the main aims in many areas of chemistry. In physical chemistry, the prediction and interpretation of structural properties and dynamic behavior of molecules are a prerequisite for a deeper understanding of their stability and chemical reactivity.[1−10] In the field of molecular spectroscopy, there is a strong relationship between the experimental outcomes and the structure of the molecular system.[11−14] Therefore, computational spectroscopy investigations often start from structural determinations. In particular, in rotational spectroscopy, the equilibrium geometry provides the major contribution to the leading terms of this technique, the rotational constants.[2,6,11] While it is seldom straightforward to derive the molecular structure from experimental information, with quantum chemistry being often required to either support or complement such determinations, state-of-the-art computational methodologies are able to provide very accurate equilibrium structures.[6,7,15,16] Indeed, in the absence of strong non-dynamical correlation effects, composite schemes rooted in the coupled-cluster model are currently able to evaluate structural parameters with an accuracy of 0.001 Å and 0.1° for bond lengths and angles, respectively.[6,17−23] However, despite the improvement in hardware and software technologies[24,25] and the increasing availability of composite schemes at reduced computational costs (e.g., the so-called "cheap" scheme and its variants),[22,26] accurate geometry optimizations are still out of range for large molecular systems due to the extremely unfavorable scaling of accurate quantum-chemical methods with the number of degrees of freedom.

A viable route is offered by the interplay of the experiment and theory in the field of rotational spectroscopy (see, e.g., refs 6,27−32). Within the so-called semi-experimental (SE) approach,[6,33] equilibrium structural parameters are derived from a least-squares fit of the SE equilibrium rotational

Received: September 3, 2021
Revised: October 20, 2021
Published: November 9, 2021

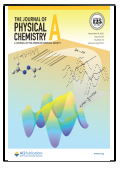

constants (B_e^{SE}) for different isotopologues. The B_e^{SE} values are obtained by correcting the experimental vibrational ground-state rotational constants[a] (B_0^{exp}) for computed vibrational contributions (ΔB_{vib}^{calc})[33]

$$B_e^{SE} = B_0^{exp} - \Delta B_{vib}^{calc} \quad (1)$$

The accuracy of this approach is well established,[27] and its application led to the definition of a database of SE equilibrium structures of small- to medium-sized semi-rigid molecules (hereafter denoted as the SE database).[29,30]

The main drawback of the SE approach is the number of experimental data required for a complete structural characterization. The greater the molecule is, the larger the number of isotopologues to be investigated becomes. Furthermore, even if the number of available B_0^{exp} constants exceeds that of the geometrical parameters to be determined, a balanced fit requires data for the isotopic substitutions involving all nuclei.[14] This becomes exceedingly difficult when the molecular size and topological complexity increase. If the number of available isotopically substituted species is not sufficient to allow a robust evaluation of all structural parameters, the lack of information can affect both the quality of the fit and their accuracy and reliability. In these cases, to avoid biased results, some geometrical parameters (i.e., those whose "experimental information" is missing) are kept fixed in the fitting procedure, usually relying on computational determinations. However, if the level of theory employed is not sufficiently high, the results of the fit and their accuracy might be unsatisfactory.[6] In this respect, powerful way-outs are offered by the template molecule (TM)[30] and/or linear regression (LR) approaches.[29]

The TM approach has been introduced to extend the size of molecular systems amenable to accurate molecular structure determinations. It is based on the idea that, if an accurate equilibrium geometry is available (either experimentally or computationally) for a smaller molecule identical to one of the system's moieties, it can be used to provide the corresponding geometrical parameters of the system under study, corrected by the differences between predictions calculated for the moieties and the system. Alternatively, the LR approach can be employed to improve the computed geometries. Indeed, within this approach, a given structural parameter is corrected by a term previously obtained from the linear regression of the fit of semi-experimental values versus the computed counterparts (at the level of theory considered) for a large set of molecules. The LR corrections are available for the most common bond distances and angles and have been collected in a database (hereafter denoted as the LR database) for several combinations of density functionals and basis sets.[29,30,34]

The idea presented in this work is to combine the TM and SE approaches, also relying on the contribution of LR corrections, with the aim of obtaining highly accurate equilibrium structures at a very reduced computational cost. The so-called TM-SE approach is based on identifying, in the molecule under study, fragments whose structures are available in the SE database mentioned above and using them to accurately determine its equilibrium geometry, possibly employing the LR approach for inter-fragment parameters (thus leading to the TM-SE_LR approach).

Among the different classes of molecular systems whose accurate structures are not yet available, one cannot overlook those issued from addition/elimination reactions of nucleophilic unsaturated radicals (e.g., CN, C_2H, and phenyl) to alkenes, imines, and aldehydes. As a matter of fact, addition of free radicals to double bonds has been studied at length because of its interest in several fields ranging from organic synthesis to atmospheric chemistry and astrochemistry (see refs 35−38 and references therein). In particular, the products of addition/elimination of free radicals to alkenes and aldehydes are well known, but accurate structures of some of them are not yet available. The situation is even more involved for imines, which—despite their low-stability under normal terrestrial conditions—play a central role in several processes, leading to the formation of the so-called complex organic molecules in the inter- and circumstellar medium (see refs 38−41 and references therein). Overall, all products of the reactions mentioned above can be seen as formed by two well-defined moieties formally linked by a single bond between two sp^2 and/or sp carbon atoms. Among the possible products, we have chosen the systems forming a suitable playground for testing the proposed TM-SE and TM-SE_LR approaches.

In the next section, the methodology is described with all details. Then, once the set of molecular systems has been introduced, the results are reported, and the validation of our approach is discussed. Examples of applications demonstrating the approach's possible extension to larger systems are also provided. Finally, concluding remarks summarize the main outcomes of this work.

METHODOLOGY

The TM-SE(_LR) approach where, for a given molecule, suitable molecular fragments are seen as "Lego bricks" is set up as follows:

- For the "Lego bricks", we resort to the TM approach, which—as mentioned in the Introduction—is based on identifying, within the molecule, "known" fragments that belong to a smaller system for which a highly accurate equilibrium geometry is available. These fragments are the TMs and are used to determine accurately the corresponding structural parameters of the larger molecular systems (r_e(lms))

$$r_e(\text{lms}) = r_e^{\text{low-cost}}(\text{lms}) + \Delta r_e(\text{TM}) \quad (2)$$

where Δr_e(TM) is defined as

$$\Delta r_e(\text{TM}) = r_e^{\text{accu}}(\text{TM}) - r_e^{\text{low-cost}}(\text{TM}) \quad (3)$$

$r_e^{\text{low-cost}}$ is the geometrical parameter of interest calculated at the same level of theory for both the molecule under consideration (lms) and the TM, the level depending on the size of the molecule to be characterized (usually a method rooted in density functional theory, DFT). A recent benchmark study[42] showed that the double-hybrid rev-DSD-PBEP86 functional[43] in conjunction with the jun-cc-pVTZ basis set[44,45] already provides rather accurate structures. Hereafter, this level of theory, shortly denoted as revDSD, will be employed for the $r_e^{\text{low-cost}}$(lms) and $r_e^{\text{low-cost}}$(TM) of eqs 2 and 3, respectively.

- Once we have the "Lego bricks", we need to put them together, the arising question being how to connect them. For this task, whenever possible, we resort to the LR approach for improving the accuracy of DFT determinations of the inter-fragment parameters. For them, the LR approach replaces the Δr_e(TM) correction

https://doi.org/10.1021/acs.jpca.1c07828
J. Phys. Chem. A 2021, 125, 9904−9916

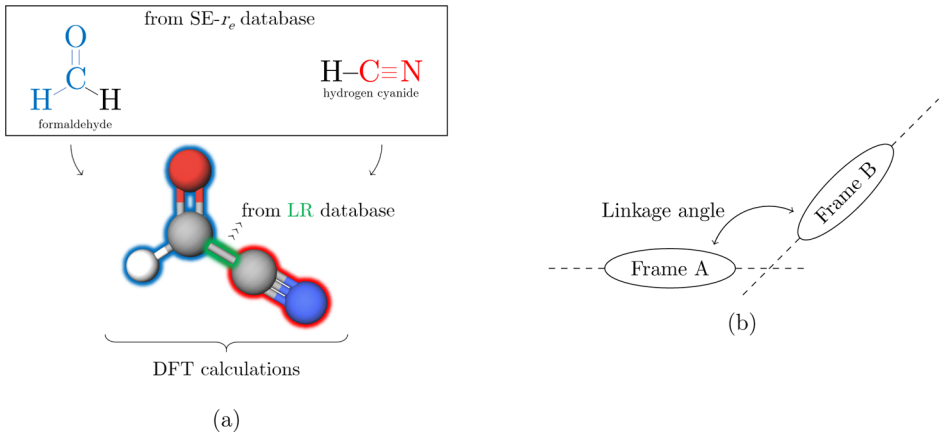

Figure 1. (a) Graphical description of the TM-SE_LR approach. (b) Definition of the linkage angle.

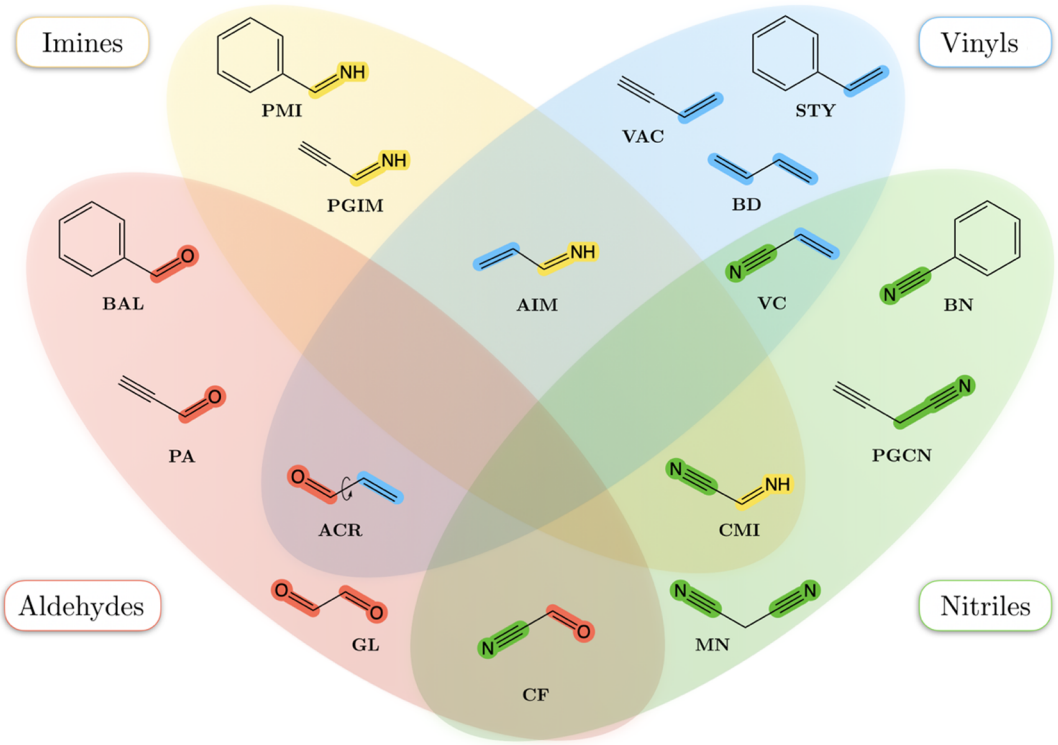

Figure 2. Dataset: molecules grouped according to their moieties, "Lego" bricks.

in eq 2 with an estimate (Δr_e(LR)) based on a linear regression model

$$\Delta r_e(\mathrm{LR}) = A r_e^{\text{low-cost}} + B \tag{4}$$

Therefore, the corrected parameter is given by

$$r_e(\mathrm{lms}) = (1 + A) r_e^{\text{low-cost}} + B \tag{5}$$

The A and B coefficients only depend on the atomic numbers of the involved atoms and were obtained by a statistical analysis of a large number of molecules. In the present context, we employ the corrective factor for the C−C (A = −0.0067 and B = 0.0069) bond length evaluated using the revDSD model and obtained from a study employing nearly 100 semi-experimental values.

If only step 1 is retained, with the linkage parameters thus kept fixed at the revDSD level, the TM-SE model is defined. The TM-SE approach is so denoted because the TMs are taken from the SE database mentioned in the Introduction. The combination of the steps 1 and 2 leads instead to the so-called TM-SE_LR approach. While in the following, we demonstrate the accuracy of the equilibrium structures "built" using the TM-SE and TM-SE_LR models, here, we note that if this approach is used to support a rotational spectroscopy study, once the latter is completed, the SE approach can be employed to refine the revDSD or LR linkage parameters, which are usually the most sensitive structural parameters.

A graphical representation of the TM-SE_LR approach is provided in Figure 1a. The example considered in this figure is formyl cyanide. In this molecule, two molecular fragments can be envisaged: the CN and HCO moieties. DFT geometry optimizations are carried out for formyl cyanide and for the TMs, namely, HCN and formaldehyde. The data available in the SE database are then used to correct the structural

https://doi.org/10.1021/acs.jpca.1c07828
J. Phys. Chem. A 2021, 125, 9904−9916

Table 1. Reference Studies Reporting the Experimental Ground-State Rotational Constants (B_0^{exp}) and Available SE Equilibrium Structures (r_e^{SE}) for the Dataset Molecules

Molecule		Ref.	Molecule		Ref.
Z-propargylimine	$\xrightarrow{B_{exp}}$	Bizzocchi et al. [54]	*trans*-acrolein	$\xrightarrow{B_{exp}}$	Jaman and Bhattacharya [55]
	$\xrightarrow{r_e^{SE}}$	This work		$\xrightarrow{r_e^{SE}}$	Puzzarini et al. [56]
E-propargylimine	$\xrightarrow{B_{exp}}$	Bizzocchi et al. [54]	*cis*-acrolein	$\xrightarrow{B_{exp}}$	Blom and Bauder [57]
Z-phenylmethanimine	$\xrightarrow{B_{exp}}$	Melli et al. [58]		$\xrightarrow{r_e^{SE}}$	Puzzarini et al. [56]
E-phenylmethanimine	$\xrightarrow{B_{exp}}$	Melli et al. [58]	cyanoformaldehyde	$\xrightarrow{B_{exp}}$	Bogey et al. [59]
Z-cyanomethanimine	$\xrightarrow{B_{exp}}$	Melosso et al. [40]	styrene	$\xrightarrow{B_{exp}}$	Caminati et al. [60]
E-cyanomethanimine	$\xrightarrow{B_{exp}}$	Melosso et al. [40]	vinylacetilene	$\xrightarrow{B_{exp}}$	Thorwirth and Lichau [61]
Z-allylimine	$\xrightarrow{B_{exp}}$	Brown et al. [62]		$\xrightarrow{r_e^{SE}}$	Thorwirth et al. [31]
E-allylimine	$\xrightarrow{B_{exp}}$	Brown et al. [62]	vinylcyanide	$\xrightarrow{B_{exp}}$	Müller et al. [63]
benzaldehyde	$\xrightarrow{B_{exp}}$	Desyatnyk et al. [64]		$\xrightarrow{r_e^{SE}}$	Thorwirth et al. [31]
propriolaldehyde	$\xrightarrow{B_{exp}}$	Jabri et al. [65]	benzonitrile	$\xrightarrow{B_{exp}}$	McGuire et al. [66]
trans-1,3-butadiene	$\xrightarrow{B_{exp}}$	Craig et al. [67]	malononitrile	$\xrightarrow{B_{exp}}$	Motiyenko et al. [68]
	$\xrightarrow{r_e^{SE}}$	Penocchio et al. [29]	propargylcyanide	$\xrightarrow{B_{exp}}$	McGuire et al. [69]
trans-glyoxal	$\xrightarrow{B_{exp}}$	Larsen et al. [70]			
	$\xrightarrow{r_e^{SE}}$	Larsen et al. [70]			

parameters of the CN and HCO moieties of formyl cyanide (see eqs 2 and 3). Finally, the DFT C−C bond distance connecting the two "Lego bricks" is corrected using the scaling factors available in the LR database.

To test the accuracy of the equilibrium structures derived using the TM-SE(_LR) approach, one can compare them with SE equilibrium geometries already available in the literature. However, this is not the best option, the TM-SE approach being designed for those cases in which the standard SE approach cannot be applied. Since rotational constants are strongly connected to molecular structures and they are experimentally determined with great accuracy,[2,6,11,27] they are the perfect means for our test. According to eq 1, to move from the ground-state to the equilibrium rotational constants and vice versa, we need the vibrational corrections, ΔB_{vib}. In the framework of vibrational perturbation theory to the second order (VPT2),[46] these are expressed as

$$\Delta B_{vib}^{i} = -\frac{1}{2}\sum_{r} \alpha_r^i \qquad (6)$$

where the α_r^i constants are the vibration−rotation interaction constants, i denotes the inertial axis, and the sum runs over all r vibrational modes. The evaluation of the α_r^i values requires anharmonic force field calculations,[14,23,27,28,32] which—in the present work—have been carried out using the global-hybrid B3LYP functional[47,48] in conjunction with the partially augmented double-ζ jun-cc-pVDZ basis set. Hereafter, this level of theory is shortly referred to as B3. Although revDSD spectroscopic parameters are usually more accurate than the B3 counterparts,[42] the ΔB_{vib} contributions benefit from a fortuitous but quite general error compensation, which allows the use of cheaper B3 computations.

All DFT calculations incorporate the D3 scheme[49] for the treatment of dispersion effects combined with the Becke-Johnson (BJ) damping function.[50] Throughout this work, all computations have been performed using the Gaussian16 suite of programs.[51]

Dataset. Before reporting and discussing the results, we need to introduce and describe the dataset employed in our study. The targeted molecules are listed in Figure 2 and have been selected following two main criteria: (1) the rotational constants of the main isotopic species are available and (2) each molecule can be envisaged as formed by two fragments, whose SE equilibrium structures are available. Going into detail, the dataset is composed of 16 species (21 molecules if isomers are considered) that result from the combination of seven fragments, namely, methanimine (CH_2NH), formaldehyde (H_2CO), hydrogen cyanide (HCN), acetylene (C_2H_2), ethene (C_2H_4), acetonitrile (CH_3CN), and benzene (C_6H_6). The SE equilibrium structures of all these fragments are available in the SE database,[29,30] the only exception being methanimine and acetonitrile, whose SE equilibrium geometries are taken from refs 52 and 53, respectively. The SE equilibrium geometries employed in this work are collected in Table S1.

The structural patterns of the chosen molecules allow their classification into four distinct and partially overlapping ensembles, depicted in Figure 2, which shows (also highlighted by different colors) the "Lego bricks" within the selected molecules. The ensemble of imines, that is, species containing the −C=NH terminal group (in yellow in Figure 2), consists of four molecules: propargylimine (PGIM), phenylmethanimine (PMI), cyanomethanimine (CMI), and allylimine (AIM). The orientation of the H atom of the −CNH moiety with respect to the other fragments of the molecule leads to the *Z* (*cis*) and *E* (*trans*) isomers. In this study, all the eight structures have been considered, the experimental rotational constants being retrieved from the reference list provided in Table 1. By replacing the imine moiety with the aldehydic −HC=O group,

https://doi.org/10.1021/acs.jpca.1c07828
J. Phys. Chem. A 2021, 125, 9904−9916

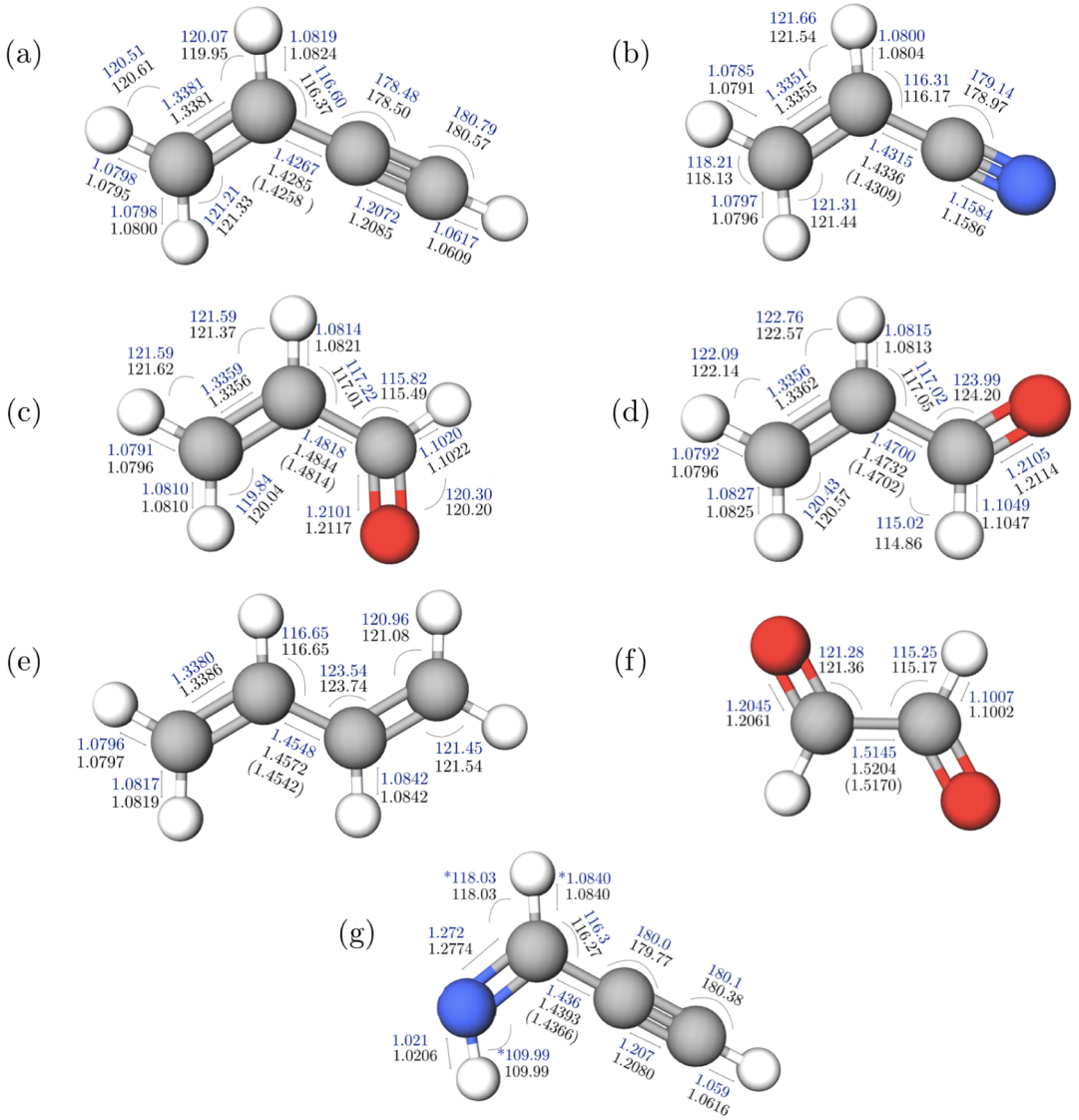

Figure 3. Molecular structures (bond lengths in angstrom and angles in degrees) of vinylacetylene (a), vinyl cyanide (b), *trans*-acrolein (c), *cis*-acrolein (d), *trans*-1,3-butadiene (e), *trans*-glyoxal (f), and *Z*-propargylimine (g). The TM-SE values are in black (for the C−C linkage bond, the TM-SE_LR value is also reported); SE parameters (errors are available in the Supporting Information, Table S2) are in blue (the asterisk denotes parameters kept fixed at the TM-SE value; the number of decimal places depends on the accuracy; see Table S2).

we obtain four molecules characterized well from an experimental point of view (see Table 1), namely, benzaldehyde (BAL), propriolaldehyde (PA), acrolein (ACR; both the *cis* and *trans* isomers), and cyanoformaldehyde (CF). The connection of two aldehydic fragments also leads to the formation of glyoxal (GL; only *trans*). They all have been collected in the red ensemble in Figure 2. Four molecules, namely, styrene (STY), vinylacetylene (VAC), 1,3-butadiene (BD; only the *trans* form), and vinyl cyanide (VC), have been selected to incorporate the vinyl $-CHCH_2$ group in the studied set of molecules, this being the light-blue set. Finally, three molecules containing the cyano −CN group, namely, benzonitrile (BN), malononitrile (MN), and propalgylcyanide (PGCN), have also been considered. The nitrile color code is green.

With the exception of MN and PGCN, all molecules present, as a linkage bond, a single CC bond connecting two unsaturated systems, and thus, non-negligible conjugation effects are expected. Therefore, the selected molecules provide a challenging test suite to validate the TM-SE model and, especially, the TM-SE_LR approach. Some molecular species present a certain degree of flexibility, which is another challenging aspect for our strategy. In particular, the two non-conjugated molecules, that is, MN and PGCN, should be good test cases with their C−C−C frame.

In Table 1, together with the list of the reference studies for the selected molecules, the references for the available SE equilibrium structures are also reported.

RESULTS AND DISCUSSION

Let us start our discussion by comparing the molecular structures issued from the TM-SE and TM-SE_LR approaches with the SE equilibrium geometries (r_e^{SE}) available in the literature for VAC, VC, *trans*-acrolein (*t*-ACR), *cis*-acrolein (*c*-ACR), *trans*-1,3-butadiene (*t*-BD), *trans*-glyoxal (*t*-GL), and *Z*-propargylimine (*Z*-PGIM). The r_e^{SE} structures of *t*-ACR and *c*-ACR have been taken from ref 56 and those of *t*-GL have been taken from ref 70; they are also available in the SE database[29]

https://doi.org/10.1021/acs.jpca.1c07828
J. Phys. Chem. A 2021, 125, 9904−9916

Table 2. Comparison of Computed Equilibrium Rotational Constants (in MHz) with the SE Counterparts for Vinylacetylene, Vinyl Cyanide, *trans*-Acrolein, *cis*-Acrolein, *trans*-1,3-Butadiene, *trans*-Glyoxal, and *Z*-Propargylimine[a]

	revDSD	TM-SE	TM-SE_LR	TM-SE_LR + corr[b]	SE(r_e^{SE})	SE(B_e^{SE})-B3[c]	SE(B_e^{SE})-CC[d]
vinylacetylene							
A_e	50611.7 (+0.39%)	50741.1 (+0.65%)	50751.6 (+0.67%)	50552.9 (+0.28%)	50413.9	50602.3 (+188.4)	50425.4 (+11.5)
B_e	4730.2 (−0.59%)	4738.2 (−0.42%)	4745.9 (−0.26%)	4752.6 (−0.12%)	4758.2	4759.4 (+1.2)	4758.0 (−0.2)
C_e	4325.9 (−0.50%)	4333.5 (−0.33%)	4340.1 (−0.18%)	4344.2 (−0.08%)	4347.8	4350.1 (+2.3)	4347.6 (−0.2)
vinyl cyanide							
A_e	50115.1 (+0.35%)	50250.1 (+0.62%)	50262.7 (+0.64%)	50071.7 (+0.27%)	49939.0	49893.3 (−45.6)	49943.9 (+4.9)
B_e	4955.5 (−0.64%)	4967.0 (−0.41%)	4975.5 (−0.24%)	4982.8 (−0.09%)	4987.3	4986.5 (−0.8)	4987.3 (+0.0)
C_e	4509.6 (−0.55%)	4520.2 (−0.31%)	4527.4 (−0.15%)	4531.9 (−0.06%)	4534.4	4533.3 (−1.1)	4534.5 (+0.1)
trans-acrolein							
A_e	47786.8 (−0.15%)	47934.4 (+0.15%)	47996.9 (+0.28%)	47899.1 (+0.08%)	47860.9	47857.9 (−2.1)	47836.7 (−23.3)
B_e	4660.4 (−0.58%)	4667.9 (−0.42%)	4675.5 (−0.26%)	4680.3 (−0.16%)	4687.8	4685.0 (−2.8)	4688.2 (+0.4)
C_e	4246.3 (−0.55%)	4253.7 (−0.37%)	4260.5 (−0.21%)	4263.7 (−0.14%)	4269.6	4267.9 (−1.7)	4270.2 (+0.6)
cis-acrolein							
A_e	22938.3 (+0.19%)	23009.8 (+0.50%)	23010.0 (+0.50%)	22971.9 (−0.10%)	22895.7	22896.4 (+0.7)	22892.8 (−2.9)
B_e	6228.5 (−1.12%)	6235.5 (−1.01%)	6250.2 (−0.78%)	6263.0 (−0.57%)	6299.1	6295.8 (−3.2)	6303.3 (+4.2)
C_e	4898.4 (−0.83%)	4906.0 (−0.69%)	4915.1 (−0.50%)	4921.3 (−0.38%)	4940.0	4939.4 (−0.6)	4943.4 (+3.4)
trans-1,3-butadiene							
A_e	42069.0 (−0.10%)	42190.6 (+0.19%)	42239.2 (+0.30%)	42123.9 (+0.03%)	42111.2	42127.1 (+16.0)	
B_e	4441.7 (−0.46%)	4445.0 (−0.38%)	4451.8 (−0.23%)	4459.7 (−0.05%)	4462.1	4460.6 (−1.4)	
C_e	4017.5 (−0.42%)	4021.3 (−0.33%)	4027.3 (−0.18%)	4032.7 (−0.05%)	4034.6	4034.3 (−0.3)	
trans-glyoxal							
A_e	55888.5 (−0.51%)	56092.7 (−0.15%)	56183.9 (+0.01%)	55973.2 (−0.36%)	56177.3	55955.7 (−221.6)	56007.1 (−170.2)
B_e	4781.5 (−0.80%)	4792.6 (−0.57%)	4802.1 (−0.37%)	4811.6 (−0.17%)	4819.9	4821.0 (+1.1)	4819.9 (0.0)
C_e	4404.7 (−0.68%)	4415.4 (−0.53%)	4423.9 (−0.34%)	4430.7 (−0.19%)	4439.1	4439.0 (−0.1)	4439.0 (−0.1)
Z-propargylimine							
A_e	54707.3 (−0.57%)	54894.9 (−0.23%)	54904.5 (−0.21%)	54690.0 (−0.61%)	55022.9	55040.7 (+17.8)	
B_e	4850.0 (−0.68%)	4858.9 (−0.50%)	4867.2 (−0.33%)	4873.9 (−0.19%)	4883.4	4883.2 (−0.2)	
C_e	4455.1 (−0.68%)	4463.8 (−0.48%)	4470.8 (−0.33%)	4475.1 (−0.23%)	4485.5	4484.2 (−1.3)	

[a]The relative differences with respect to SE(r_e^{SE}) are reported within parentheses. [b]Correction of −0.2° on the linkage angle. Referring to Figure 1b, the minus sign denotes a lowering of the linkage angle. [c]SE(B_e^{SE}) using vibrational corrections at the B3 level. The difference SE(B_e^{SE}) − SE(r_e^{SE}) is reported within parentheses. [d]SE(B_e^{SE}) using vibrational corrections at the fc-CCSD(T)/cc-pVTZ level [from ref 31 for VAC and VC, from ref 56 for ACR (*trans* and *cis*), and from ref 70 for *t*-GL]. The difference SE(B_e^{SE}) − SE(r_e^{SE}) is reported within parentheses.

together with the r_e^{SE} of *t*-BD. Those of VC and VAC were evaluated in ref 31 and that of *Z*-PGIM has been purposely determined in this work using the data from refs 54 and 71. For *Z*-PGIM, the availability, in addition to the rotational constants of the parent isotopologues, of the data for the three ^{13}C isotopic species and two deuterated variants (at the −NH and −CCH sites) has enabled a reliable, even if partial, determination of the SE equilibrium structure.

Figure 3 shows the molecular structures of the seven test cases, also providing the comparison between the TM-SE_LR and SE equilibrium geometries. These are also collected in Table S2 of the Supporting Information together with the uncertainties affecting the r_e^{SE} structures and the revDSD structural parameters. The fragments employed in the TM-SE are evident: ethylene and acetylene for VAC, ethylene and hydrogen cyanide for VC, ethylene and formaldehyde for *t*-ACR and *c*-ACR, ethylene for *t*-BD, formaldehyde for *t*-GL, and methanimine and acetylene for *Z*-PGIM. Their revDSD and SE structural parameters are collected in Table S1 of the Supporting Information. From Figure 3, a very good agreement between the TM-SE(_LR) and r_e^{SE} geometries is apparent. It is noted that the deviations are in the order of 0.001 Å for bond lengths and 0.1° for angles. There are only a very few exceptions showing discrepancies larger than 0.001 Å (but always within 2 mÅ), and these can be ascribed to conjugative effects. While the revDSD level already provides good results (deviations in the order of +0.003 Å for bond lengths and |0.2|° for angles; see Table S2 of the Supporting Information), the improvement provided by the TM-SE approach is apparent. The only somewhat uncertain comparison concerns *Z*-PGIM, for which the experimental data are not sufficient for a complete structural determination. At this point, it is interesting to check how the small discrepancies observed in the structural parameters reflect on the rotational constants, the results being reported in Table 2. Indeed, rotational constants are extremely sensitive to the molecular structure. In fact, variations of 0.001 Å in the bond distances and 0.1° in valence angles can lead to changes up to ±50 MHz for the *A* constant and ±15 MHz for *B* and *C*. This issue is very important because the first application we have in mind is the prediction of the rotational spectra of "unknown" molecules with a very good accuracy at a limited computational cost.

In Table 2, the equilibrium rotational constants straightforwardly derived from the r_e^{SE} structures are denoted as SE(r_e^{SE}). For comparison purposes, those derived from the experimental ground-state rotational constants corrected for the vibrational contributions at the B3 level are also reported, these being denoted as SE(B_e^{SE})-B3. For VAC, VC, *t*-ACR, *c*-ACR, and *t*-GL, the SE(B_e^{SE}) values obtained using vibrational corrections at the fc-CCSD(T)/cc-pVTZ[44] level available in the literature[30,31] are also given (SE(B_e^{SE})-CC). CCSD(T)[72] denotes the coupled-cluster single and double approximation augmented by a perturbative treatment of triples, and fc stands

https://doi.org/10.1021/acs.jpca.1c07828
J. Phys. Chem. A 2021, 125, 9904−9916

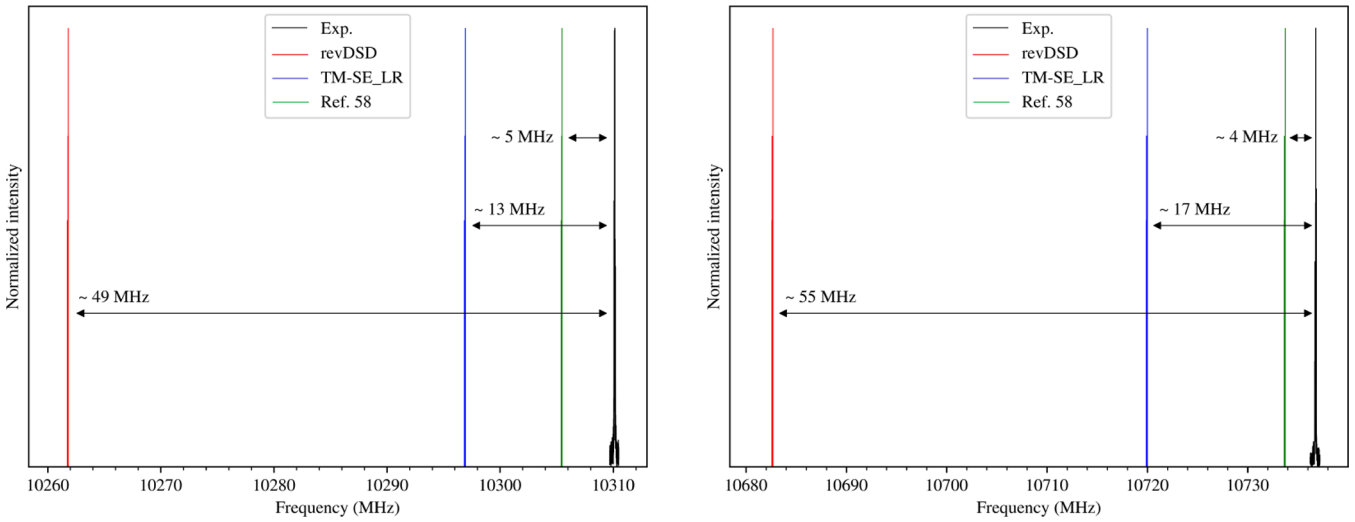

Figure 4. Comparison between the experimental spectrum (Exp.) and different simulations (revDSD, TM-SE_LR, and "cheap" scheme from ref 58) for both isomers of PMI. The $4_{1,4} \leftarrow 3_{1,3}$ transition of *E*-PMI (left panel) and the $4_{0,4} \leftarrow 3_{0,3}$ transition of *Z*-PMI (right panel) have been chosen as examples ($J_{K_a,K_c} \leftarrow J'_{K'_a,K'_c}$).

for the frozen-core approximation. The comparison between these two sets of SE B_e constants is crucial because for the other molecules of the dataset, the performance of the TM-SE(_LR) approach will be based on the latter type of SE B_e values. In principle, the two routes should lead to equivalent results. However, we note that vibrational corrections at the CCSD(T) level tend to provide a better agreement, with the average discrepancy being, in relative terms, ∼0.04%. When B3 vibrational corrections are considered, the differences are a bit larger, but the mean deviation is still as low as 0.06%. We note a few large discrepancies from the SE(r_e^{SE}) values, all for the *A* constant. When considering the B3 vibrational corrections, the largest deviations are 0.37% for VAC and 0.40% for *t*-GL. In the case of CCSD(T) vibrational corrections, the only outlier is observed for *t*-GL, the deviation being 0.30%. If we exclude these data, the relative averaged discrepancies from SE(r_e^{SE}) reduce to 0.02% for CCSD(T) and 0.03% for B3. This comparison provides a quantification of the systematic error affecting our analysis. Conservatively, we consider that the SE equilibrium rotational constants employed in the analysis of the dataset (i.e., those obtained with B3 vibrational corrections) are affected by a systematic uncertainty well within 0.1%. At this point, the accuracy of the SE equilibrium structure deserves a note. While the limited accuracy of the B3 vibrational corrections affects, even if marginally, the derived SE equilibrium rotational constants, the effects are entirely negligible on the structural determination, as demonstrated well by the literature on this topic; for example, see refs 27 and 30.

Before discussing the results of Table 2, it should be pointed out that the accuracy reached by the TM-SE and TM-SE_LR models can only be approached by applying expensive accurate composite schemes based on coupled-cluster theory.[2,5,73,74] An example is provided by the experimental investigation on the rotational spectrum of propargylimine, which also led to its detection in the interstellar medium.[54] In that work, the spectroscopic study was supported by quantum-chemical calculations, with equilibrium rotational constants obtained by means of the so-called "CCSD(T)/CBS + CV" composite scheme,[19,20] whose accuracy has been tested in refs 2 and 73. This composite scheme exploits the CCSD(T) method extrapolated to the complete basis set (CBS) limit (within the fc approximation) and incorporates the core-valence (CV) correlation correction. The CCSD(T)/CBS + CV B_e constants are 54525.7, 4876.6, and 4476.3 MHz, which deviate from the SE counterparts by 0.90, 0.14, and 0.21%, respectively, to be compared with those issuing from the TM-SE_LR model, which differ instead by 0.21, 0.33, and 0.33% (see Table 2). Another example is provided by ACR, which points out how accurate the CCSD(T)/CBS + CV composite scheme can be. In ref 56, this approach was employed in the geometry optimization of *t*- and *c*-ACR. The corresponding equilibrium rotational constants (22915.2, 6301.4, and 4942.3 MHz for *c*-ACR and 47870.0, 4689.3, and 4270.9 MHz for *t*-ACR) were found to deviate, on average, by only 0.04% from the SE(r_e^{SE}) values.

From the comparisons of Table 2, we note that—for all test cases—the deviations are small at all the levels considered, with an overall improvement when moving from revDSD to TM-SE. A further improvement is noted by resorting to the TM-SE_LR approach. In more detail, the absolute mean deviations from the SE(r_e^{SE}) values are 0.5% at the revDSD level, 0.4% for TM-SE, and 0.3% for TM-SE_LR. In several cases, as already noted in the comparison between SE(r_e^{SE}) and SE(B_e^{SE}) and well-known in the literature (see, e.g., ref 74), the agreement for the *A* constant is the most critical among the three rotational constants. Indeed, it worsens when moving from the revDSD level to the TM-SE approach, with the LR corrections being unable to improve this discrepancy. An inspection of the revDSD, SE, and TM-SE structures revealed that this is caused by very small structural modifications, and in detail, it seems to be due to missing LR corrections for linkage angles (see Figure 1b for the definition). Actually, the LR terms are available for angles, but the inter-fragment angles tend to behave differently. They somewhat resemble the intermolecular angles in non-covalent complexes. While this might be a sort of limitation in predicting the rotational constants and the corresponding spectrum of an "unknown" molecule with high accuracy, once the latter is assigned and analyzed, the experimental rotational constants of just one isotopic species are sufficient to effectively correct the linkage parameters and lead to an equilibrium structure of great accuracy. For example,

https://doi.org/10.1021/acs.jpca.1c07828
J. Phys. Chem. A 2021, 125, 9904−9916

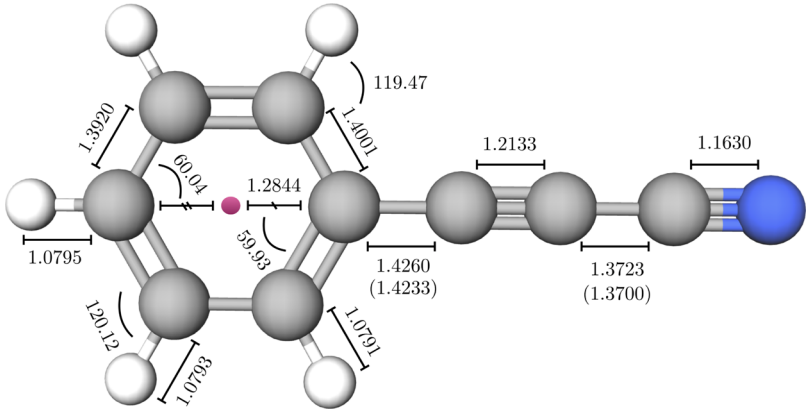

Figure 5. Structural parameters of 3-phenyl-2-propynenitrile obtained with the TM-SE and TM-SR_LR approaches. The two values in parentheses refer to LR-corrected C−C bond distances. All bond lengths are in Å, and angles are in degrees.

if we consider *Z*-CMI and refine the revDSD linkage parameters (the C−C distance and the corresponding angle) using the experimental rotational constants of the main isotopic species (the only ones investigated so far), the discrepancies with respect to the SE B_e^{SE} values reduce to −0.02, 0.001, and 0.002% for *A*, *B*, and *C*, respectively, with these being −0.21, −0.49, and −0.47%, respectively, at the TM-SE level (see Table S3). Even if we only fit the C−C linkage bond, the resulting discrepancies are extremely good: −0.15, 0.006, and 0.004%, respectively.

For the seven molecules under consideration, tests have been carried out in order to understand if a systematic corrective term can be applied to the linkage angle (see Figure 1b). The outcome of these tests (see the fourth column of Table 2) suggests that indeed, a lowering of 0.2° improves the agreement of the TM-SE_LR rotational constants with respect to the SE ones, with the only exception of the A rotational constant of *t*-GL and *Z*-PGIM. Such an improvement leads to a reduction in the absolute mean deviation to 0.2%. Interestingly, for *Z*-PGIM, an additional correction (−0.002 Å) to the C−C LR corrective term leads to an improvement for all rotational constants: 54911.6 MHz (−0.20%), 4873.3 MHz (−0.21%), and 4476.1 MHz (−0.21%). These results seem to suggest that the LR correction is not entirely able to recover conjugative effects due to double and triple bonds connected to the C−C single linkage. Such a limitation is also expected for *c*-ACR, for which the deviations on *B* and *C* are rather significant for all levels of theory, for example, from −1.12% for B at the revDSD level to −0.78% for TM-SE_LR. While the additional corrective term works well for all imines, we anticipate that the "−0.2° correction" extended to the entire dataset works fine only for the molecules containing the vinyl frame (see Table S3).

As mentioned in the Methodology section, the TM-SE and TM-SE_LR approaches have been extended to the dataset introduced above. The results are collected in Table S3 of the Supporting Information, where the revDSD, TM-SE, and TM-SE_LR equilibrium rotational constants are compared with the SE(B_e^{SE}) constants obtained from the experimental ground-state rotational constants (B_0^{exp}) and the B3 vibrational corrections. The B_0^{exp} constants and the corresponding ΔB_{vib}^{B3} corrections are reported in Table S3, which also collects the TM-SE_LR + corr results, evaluated as explained and addressed above.

From the inspection of Table S3, results in line with those of Table 2 are noted. In almost all cases, the revDSD level provides relative deviations with respect to the B_e^{SE} values within 1%. The use of the TM-SE approach improves the agreement in almost all cases, with an average relative deviation of 0.3%. A further improvement is noted once the LR corrections are considered (TM-SE_LR approach), the average relative deviation reducing to 0.2%. Based on the accuracy of the SE equilibrium rotational constants discussed above, the relative error of the TM-SE_LR rotational constants can be—on average—as low as 0.1%. Such a good agreement on the SE B_e constants implies that the TM-SE_LR structures are highly accurate, which means average deviations smaller than 0.001 Å for bond lengths and 0.1° for angles. Finally, we note that the more rigid the molecule is, the better the TM-SE approach works, as demonstrated—for example—by phenylmethanimine and benzonitrile.

Rotational Spectrum of Phenylmethanimine. As mentioned above, the TM-SE approach is particularly accurate for rigid molecular systems. To demonstrate this outcome, we applied it to the simulation of the rotational spectrum of *E*- and *Z*-PMI. For this purpose, the ground-state rotational constants have been predicted by adding the B3 vibrational corrections to the revDSD and TM-SE_LR equilibrium values (according to eq 1). To complete the set of the required spectroscopic parameters, namely, the quartic centrifugal-distortion and nitrogen quadrupole-coupling constants, we refer to the computational results reported in ref 58.

The comparison is shown in Figure 4 by means of two selected rotational transitions, one for *E*-PGIM and one for *Z*-PGIM. It is apparent that the TM-SE_LR approach leads to a significant improvement with respect to the starting revDSD level; indeed, the error associated to the transition frequency decreases by about three times. For the sake of completeness, the prediction based on the "cheap" composite scheme (from ref 58: "best theo" column of Table 1) has also been considered. It is noted that the latter (green stick spectra in Figure 4) is the most accurate; however, such a good agreement comes at the price of a much greater computational cost. In fact, the "cheap" composite scheme[22] is based on the CCSD(T) method. Furthermore, for the specific case of PGIM, the latter approach showed an extraordinarily good agreement. Therefore, this example confirms that the TM-SE_LR approach is able to provide a remarkable accuracy in rotational spectral predictions, without increasing the compu-

https://doi.org/10.1021/acs.jpca.1c07828
J. Phys. Chem. A 2021, 125, 9904−9916

Table 3. Comparison between Computed Equilibrium Rotational Constants (in MHz) and the SE Counterparts for 3-Phenyl-2-propynenitrile[a]

	B_e				
	revDSD	TM-SE	TM-SE_LR	SE[b]	B_0^{exp} [ΔB_{vib}^{B3}]
A	5681.4 (−0.35%)	5703.0 (+0.01%)	5702.0 (+0.01%)	5701.4	5659.722(15) [41.6]
B	568.5 (−0.41%)	569.9 (−0.16%)	570.7 (−0.02%)	570.8	569.582206(39) [1.2]
C	516.8 (−0.41%)	518.1 (−0.15%)	518.8 (−0.01%)	518.9	517.404488(37) [1.5]

[a]The relative differences with respect to SE(B_e^{SE}) are reported in parentheses. [b]Ground-state rotational constants from ref 75 corrected for vibrational corrections at the B3 level.

Table 4. Prediction of Rotational Constants (in MHz) of *o*-, *m*-, and *p*-cyanoethynylbenzene

	B_e (revDSD)	B_e (TM-SE)	B_e (TM-SE_LR)	ΔB_{vib}	B_0 (TM-SE_LR)[a]
o-CEB					
A	2025.1	2031.0	2033.00	4.66	2028.34
B	1330.2	1334.0	1335.48	6.11	1329.37
C	802.9	805.1	806.01	3.23	802.78
m-CEB					
A	2707.1	2715.4	2717.55	10.44	2707.11
B	906.6	909.0	910.16	3.47	906.69
C	679.1	681.0	681.81	2.80	679.01
p-CEB					
A	5673.0	5693.2	5693.19	45.85	5647.34
B	708.5	710.3	711.29	2.19	709.10
C	629.9	631.5	632.29	2.31	629.98

[a]B_e(TM-SE_LR) constants augmented by B3 vibrational corrections.

tational effort with respect to revDSD. It is thus more than suitable for guiding and supporting experimental studies.

Structure of 3-Phenyl-2-propynenitrile and Its Isomers. During the preparation of this manuscript, we became aware of the spectroscopic characterization of 3-phenyl-2-propynenitrile (PPN).[75] Since—as noted above—the TM-SE approach works extremely well for rather rigid molecules, we decided to apply it to the structural determination of PPN and its isomers, thus providing an example of extension of the TM-SE approach to a larger system. For PPN, the resulting structure is shown in Figure 5, with the corresponding rotational constants being collected in Table 3. To build the PPN molecule, three fragments have been actually employed in the TM-SE approach: the phenyl moiety from benzene, the −C≡C− group from acetylene, and the −CN frame from HCN. Within the TM-SE_LR approach, the LR correction has been applied to the two C−C linkage bonds. All details can be found in Table S4 of the Supporting Information.

From the inspection of Table 3, it is evident that—as expected—the TM-SE approach is able to predict accurate equilibrium rotational constants, which in turn means an accurate equilibrium structure. In particular, the results for the TM-SE_LR model are really impressive. Indeed, we note that going from revDSD to TM-SE leads to a reduction in the average relative error from 0.4 to 0.1%. Then, incorporation of the LR corrections further decreases the average relative deviation to 0.01%. In view of such a good performance, the TM-SE approach can be used to predict with great accuracy the rotational constants of different isomers of PPN: *o*-, *m*-, and *p*-cyanoethynylbenzene (CEB; see Table 4). Based on the analysis carried out in this manuscript and—in particular—for PPN, we expect that the equilibrium rotational constants issued from the TM-SE_LR approach have a relative accuracy well within 0.05%. Using the ground-state rotational constants of Table 4, the rotational spectra of *o*-, *m*-, and *p*-CEB have been simulated and are shown in Figure 6. For all the three molecules, the *a*-type transitions are the most intense and reach the maximum intensity in the millimeter-wave region, between 170 and 220 GHz. In this frequency region, the accuracy of the predicted rotational transitions is expected to range between 200 and 400 MHz, also accounting for the uncertainties affecting the computed centrifugal distortion constants (which are required for spectral predictions).

CONCLUSIONS

A benchmark study based on the availability of accurate semi-experimental equilibrium rotational constants for 21 molecular species allowed us to demonstrate the reliability, robustness, and accuracy of a "Lego brick" approach, the so-called TM-SE approach. For the selected molecules, each species has been seen as formed by two fragments, the "Lego bricks", for which accurate semi-experimental structures are available. Accounting, at the rev-DSD-PBEP86-D3/jun-cc-pVTZ level, for the modifications taking place when moving from the isolated fragments to the molecular species of interest leads to the definition of the TM-SE equilibrium structure. A further improvement has been obtained by correcting the inter-fragment parameters with the linear regression corrective terms available for rev-DSD-PBEP86-D3/jun-cc-pVTZ. The resulting structure has been denoted as TM-SE_LR. For the TM-SE and TM-SE_LR equilibrium rotational constants, the average relative deviation with respect to accurate semi-experimental equilibrium rotational constants has been found to be ∼0.3 and ∼0.2%, respectively. According to the thorough investigation of the equilibrium geometries of 7 from the 21 molecules, these discrepancies reflect structural differences of about 0.001 Å for bond lengths and 0.1° for angles.

In conclusion, since the only quantum-chemical calculations required by the TM-SE and TM-SE_LR models are geometry optimizations at the rev-DSD-PBEP86-D3/jun-cc-pVTZ level,

https://doi.org/10.1021/acs.jpca.1c07828
J. Phys. Chem. A 2021, 125, 9904−9916

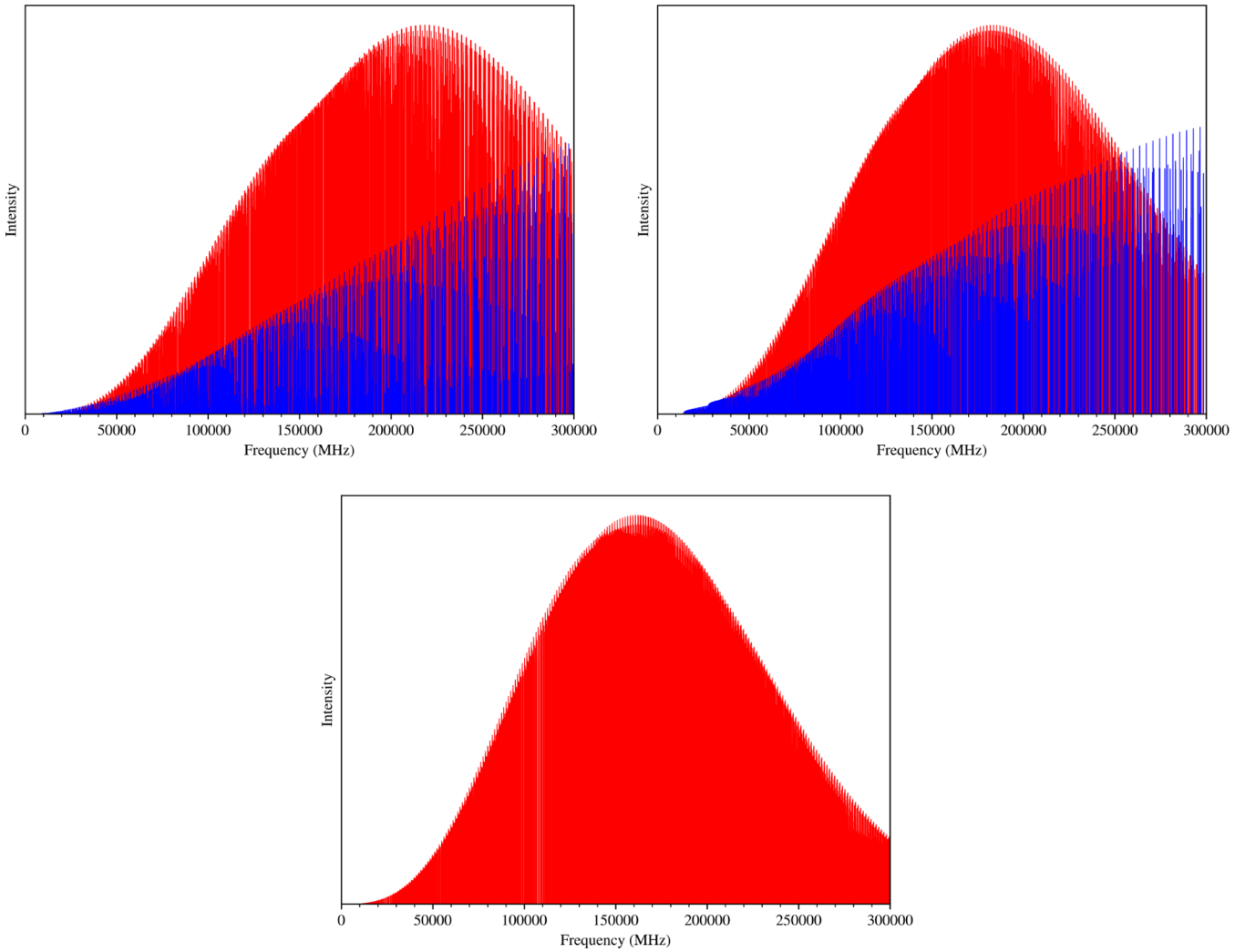

Figure 6. Simulation of the rotational spectrum of *o*- (top-left panel), *m*- (top-right panel), and *p*-CEB (bottom panel). The red and blue sticks represent the *a*- and *b*-type transitions, respectively.

they are low-cost approaches able to provide an accuracy close to that of the most sophisticated composite approaches based on the coupled-cluster ansatz. Therefore, they are very promising tools for the accurate structural characterizations of medium- to large-sized molecular systems, such as the building blocks of biological molecules. Interestingly, test computations on a reduced dataset showed that the application of the TM-SE approach to B3-optimized geometries nearly doubles the relative deviations from the semi-experimental equilibrium rotational constants, thus implying a limited worsening in the structural parameters with respect to the models discussed above.

Finally, the TM-SE(_LR) approach is also suited well for unstable species of medium to large dimensions, which are of current interest in many different fields, ranging from astrochemistry to biochemistry, and whose structures can be hardly determined by experiments. Furthermore, our test on 3-phenyl-2-propynenitrile points out that the TM-SE(_LR) approach can be reliably extended to more than two "Lego bricks", while the availability of LR corrections for bond lengths other than the C−C bond ones opens to its application to a wider range of molecular species.

■ ASSOCIATED CONTENT

Supporting Information

The Supporting Information is available free of charge at https://pubs.acs.org/doi/10.1021/acs.jpca.1c07828.

Table S1. Template molecules: revDSD and semi-experimental equilibrium structures. Table S2: comparison between the semi-experimental and computed (revDSD, TM-SE, and TM-SE_LR) values of the structural parameters of vinylacetylene, vinyl cyanide, (*cis*, *trans*)-acrolein, *trans*-1,3-butadiene, *trans*-glyoxal, and *Z*-propargylimine. Table S3: computed equilibrium rotational constants and the SE counterparts together with the ground-state rotational constants and the corresponding vibrational corrections for the molecules of the dataset. Table S4: computed and template values of the structural parameters of 3-phenyl-2-propynenitrile and its isomers (*o*-, *m*-, and *p*-cyanoethynylbenzene) (PDF)

https://doi.org/10.1021/acs.jpca.1c07828
J. Phys. Chem. A 2021, 125, 9904−9916

AUTHOR INFORMATION

Corresponding Authors

Vincenzo Barone − *Scuola Normale Superiore, 56126 Pisa, Italy;* orcid.org/0000-0001-6420-4107; Email: vincenzo.barone@sns.it

Cristina Puzzarini − *Dipartimento di Chimica "Giacomo Ciamician", Università di Bologna, 40126 Bologna, Italy;* orcid.org/0000-0002-2395-8532; Email: cristina.puzzarini@unibo.it

Authors

Alessio Melli − *Scuola Normale Superiore, 56126 Pisa, Italy; Dipartimento di Chimica "Giacomo Ciamician", Università di Bologna, 40126 Bologna, Italy;* orcid.org/0000-0002-8469-1624

Francesca Tonolo − *Scuola Normale Superiore, 56126 Pisa, Italy; Dipartimento di Chimica "Giacomo Ciamician", Università di Bologna, 40126 Bologna, Italy*

Complete contact information is available at: https://pubs.acs.org/10.1021/acs.jpca.1c07828

Author Contributions

[§]A.M. and F.T. contributed equally to this paper.

Notes

The authors declare no competing financial interest.

ACKNOWLEDGMENTS

This work has been supported by the MIUR (grant number 2017A4XRCA) and by the University of Bologna (RFO funds). The SMART@SNS Laboratory (http://smart.sns.it) is acknowledged for providing high-performance computing facilities.

ADDITIONAL NOTE

[a]Note that for a given isotopic species, the number of rotational constants depends on the rotational symmetry. At most, there are three of them in the case of asymmetric rotors.

REFERENCES

(1) Domenicano, A.; Hargittai, I.. *Accurate Molecular Structures: Their Determination and Importance*; Oxford University Press, 1992; Vol. *1*.

(2) Puzzarini, C.; Heckert, M.; Gauss, J. The accuracy of rotational constants predicted by high-level quantum-chemical calculations. I. Molecules containing first-row atoms. *J. Chem. Phys.* **2008**, *128*, 194108.

(3) Caminati, W.; Grabow, J.-U. Microwave Spectroscopy. In *Frontiers of Molecular Spectroscopy*; Laane, J., Ed.; Elsevier: Amsterdam, 2009; Chapter 15, pp 455−552.

(4) Puzzarini, C. Rotational spectroscopy meets theory. *Phys. Chem. Chem. Phys.* **2013**, *15*, 6595−6607.

(5) Puzzarini, C. Accurate molecular structures of small- and medium-sized molecules. *Int. J. Quantum Chem.* **2016**, *116*, 1513−1519.

(6) Demaison, J.; Boggs, J. E.; Császár, A. G.. *Equilibrium Molecular Structures: From Spectroscopy to Quantum Chemistry*; CRC Press, 2016.

(7) Puzzarini, C.; Barone, V. Diving for accurate structures in the ocean of molecular systems with the help of spectroscopy and quantum chemistry. *Acc. Chem. Res.* **2018**, *51*, 548−556.

(8) Pate, B. H.; Evangelisti, L.; Caminati, W.; Xu, Y.; Thomas, J.; Patterson, D.; Perez, C.; Schnell, M. Quantitative Chiral Analysis by Molecular Rotational Spectroscopy. In *Chiral Analysis*, 2nd ed.; Polavarapu, P. L., Ed.; Elsevier, 2018; Chapter 17, pp 679−729.

(9) Graziano, G. Fingerprints of molecular reactivity. *Nat. Rev. Chem.* **2020**, *4*, 227.

(10) Arnaut, L. Relationships between structure and reactivity. In *Chemical Kinetics*, 2nd ed.; Arnaut, L., Ed.; Elsevier, 2021; Chapter 7, pp 225−245.

(11) Gordy, W.; Cook, R. L. *Microwave Molecular Spectra*; Wiley, 1984.

(12) Jensen, P.; Bunker, P. R. *Computational Molecular Spectroscopy*; John Wiley & Sons: U.K., 2000.

(13) *Computational Strategies for Spectroscopy: from Small Molecules to Nano Systems*; Barone, V., Ed.; John Wiley & Sons, Inc., 2011.

(14) Puzzarini, C.; Stanton, J. F.; Gauss, J. Quantum-chemical calculation of spectroscopic parameters for rotational spectroscopy. *Int. Rev. Phys. Chem.* **2010**, *29*, 273−367.

(15) Puzzarini, C.; Barone, V. Toward spectroscopic accuracy for organic free radicals: Molecular structure, vibrational spectrum, and magnetic properties of F2NO. *J. Chem. Phys.* **2008**, *129*, 084306.

(16) Heim, Z. N.; Amberger, B. K.; Esselman, B. J.; Stanton, J. F.; Woods, R. C.; McMahon, R. J. Molecular structure determination: Equilibrium structure of pyrimidine (m-C4H4N2) from rotational spectroscopy (reSE) and high-level ab initio calculation (re) agree within the uncertainty of experimental measurement. *J. Chem. Phys.* **2020**, *152*, 104303.

(17) Martin, J. M. L.; Taylor, P. R. The geometry, vibrational frequencies, and total atomization energy of ethylene. A calibration study. *Chem. Phys. Lett.* **1996**, *248*, 336−344.

(18) Schuurman, M. S.; Allen, W. D.; von Ragué Schleyer, P.; Schaefer, H. F., III The highly anharmonic BH5 potential energy surface characterized in the ab initio limit. *J. Chem. Phys.* **2005**, *122*, 104302.

(19) Heckert, M.; KÁllay, M.; Gauss, J. Molecular Equilibrium Geometries Based on Coupled-Cluster Calculations Including Quadruple Excitations. *Mol. Phys.* **2005**, *103*, 2109.

(20) Heckert, M.; Kállay, M.; Tew, D. P.; Klopper, W.; Gauss, J. Basis-Set Extrapolation Techniques for the Accurate Calculation of Molecular Equilibrium Geometries Using Coupled-Cluster Theory. *J. Chem. Phys.* **2006**, *125*, 044108.

(21) Puzzarini, C. Extrapolation to the complete basis set limit of structural parameters: Comparison of different approaches. *J. Phys. Chem. A* **2009**, *113*, 14530−14535.

(22) Puzzarini, C.; Barone, V. Extending the molecular size in accurate quantum-chemical calculations: The equilibrium structure and spectroscopic properties of uracil. *Phys. Chem. Chem. Phys.* **2011**, *13*, 7189−7197.

(23) Puzzarini, C.; Bloino, J.; Tasinato, N.; Barone, V. Accuracy and interpretability: The devil and the holy grail. New routes across old boundaries in computational spectroscopy. *Chem. Rev.* **2019**, *119*, 8131−8191.

(24) Cao, Y.; Romero, J.; Olson, J. P.; Degroote, M.; Johnson, P. D.; Kieferová, M.; Kivlichan, I. D.; Menke, T.; Peropadre, B.; Sawaya, N. P. D.; et al. Quantum Chemistry in the Age of Quantum Computing. *Chem. Rev.* **2019**, *119*, 10856−10915.

(25) Barone, V.; Puzzarini, C.; Mancini, G. Integration of theory, simulation, artificial intelligence and virtual reality: a four-pillar approach for reconciling accuracy and interpretability in computational spectroscopy. *Phys. Chem. Chem. Phys.* **2021**, *23*, 17079−17096.

(26) Alessandrini, S.; Barone, V.; Puzzarini, C. Extension of the "cheap" composite approach to noncovalent interactions: The jun-ChS scheme. *J. Chem. Theory Comput.* **2019**, *16*, 988−1006.

(27) Pawłowski, F.; Jørgensen, P.; Olsen, J.; Hegelund, F.; Helgaker, T.; Gauss, J.; Bak, K. L.; Stanton, J. F. Molecular equilibrium structures from experimental rotational constants and calculated vibration−rotation interaction constants. *J. Chem. Phys.* **2002**, *116*, 6482−6496.

(28) Liévin, J.; Demaison, J.; Herman, M.; Fayt, A.; Puzzarini, C. Comparison of the experimental, semi-experimental and ab initio equilibrium structures of acetylene: Influence of relativisitic effects and of the diagonal Born-Oppenheimer corrections. *J. Chem. Phys.* **2011**, *134*, 064119.

(29) Penocchio, E.; Piccardo, M.; Barone, V. Semiexperimental equilibrium structures for building blocks of organic and biological molecules: The B2PLYP route. *J. Chem. Theory Comput.* **2015**, *11*, 4689−4707.
(30) Piccardo, M.; Penocchio, E.; Puzzarini, C.; Biczysko, M.; Barone, V. Semi-experimental equilibrium structure determinations by employing B3LYP/SNSD anharmonic force fields: Validation and application to semirigid organic molecules. *J. Phys. Chem. A* **2015**, *119*, 2058−2082.
(31) Thorwirth, S.; Harding, M. E.; Dudek, J. B.; McCarthy, M. C. Equilibrium molecular structures of vinyl carbon chains: Vinyl acetylene, vinyl diacetylene, and vinyl cyanide. *J. Mol. Spectrosc.* **2018**, *350*, 10−17.
(32) Orr, V. L.; Ichikawa, Y.; Patel, A. R.; Kougias, S. M.; Kobayashi, K.; Stanton, J. F.; Esselman, B. J.; Woods, R. C.; McMahon, R. J. Precise equilibrium structure determination of thiophene (c-C4H4S) by rotational spectroscopy-Structure of a five-membered heterocycle containing a third-row atom. *J. Chem. Phys.* **2021**, *154*, 244310.
(33) Pulay, P.; Meyer, W.; Boggs, J. E. Cubic force constants and equilibrium geometry of methane from Hartree-Fock and correlated wavefunctions. *J. Chem. Phys.* **1978**, *68*, 5077−5085.
(34) Penocchio, E.; Mendolicchio, M.; Tasinato, N.; Barone, V. Structural features of the carbon-sulfur chemical bond: a semi-experimental perspective. *Can. J. Chem.* **2016**, *94*, 1065−1076.
(35) Vereecken, L.; Groof, P. D.; Peeters, J. Temperature and pressure dependent product distribution of the addition of CN radicals to C2H4. *Phys. Chem. Chem. Phys.* **2003**, *5*, 5070−5076.
(36) Tonolo, F.; Lupi, J.; Puzzarini, C.; Barone, V. The Quest for a Plausible Formation Route of Formyl Cyanide in the Interstellar Medium: a State-of-the-art Quantum-chemical and Kinetic Approach. *Astrophys. J.* **2020**, *900*, 85.
(37) Dash, M. R.; Rajakumar, B. Abstraction and addition kinetics of C2H radicals with CH4, C2H6, C3H8, C2H4, and C3H6: CVT/SCT/ISPE and hybrid meta-DFT methods. *Phys. Chem. Chem. Phys.* **2015**, *17*, 3142−3156.
(38) Lupi, J.; Puzzarini, C.; Barone, V. Methanimine as a Key Precursor of Imines in the Interstellar Medium: The Case of Propargylimine. *Astrophys. J. Lett.* **2020**, *903*, L35.
(39) Vazart, F.; Calderini, D.; Puzzarini, C.; Skouteris, D.; Barone, V. State-of-the-Art Thermochemical and Kinetic Computations for Astrochemical Complex Organic Molecules: Formamide Formation in Cold Interstellar Clouds as a Case Study. *J. Chem. Theory Comput.* **2016**, *12*, 5385−5397.
(40) Melosso, M.; Melli, A.; Puzzarini, C.; Codella, C.; Spada, L.; Dore, L.; Degli Esposti, C.; Lefloch, B.; Bachiller, R.; Ceccarelli, C.; et al. Laboratory measurements and astronomical search for cyanomethanimine. *Astron. Astrophys.* **2018**, *609*, A121.
(41) Alessandrini, S.; Tonolo, F.; Puzzarini, C. In search of phosphorus in astronomical environments: The reaction between the CP radical (X2Σ+) and methanimine. *J. Chem. Phys.* **2021**, *154*, 054306.
(42) Barone, V.; Ceselin, G.; Fusè, M.; Tasinato, N. Accuracy meets interpretability for computational spectroscopy by means of hybrid and double-hybrid functionals. *Front. Chem.* **2020**, *8*, 584203.
(43) Santra, G.; Sylvetsky, N.; Martin, J. M. L. Minimally empirical double-hybrid functionals trained against the GMTKN55 database: revDSD-PBEP86-D4, revDOD-PBE-D4, and DOD-SCAN-D4. *J. Phys. Chem. A* **2019**, *123*, 5129−5143.
(44) Dunning, T. H. Gaussian basis sets for use in correlated molecular calculations. I. The atoms boron through neon and hydrogen. *J. Chem. Phys.* **1989**, *90*, 1007−1023.
(45) Papajak, E.; Truhlar, D. G. Convergent Partially Augmented Basis Sets for Post-Hartree−Fock Calculations of Molecular Properties and Reaction Barrier Heights. *J. Chem. Theory Comput.* **2011**, *7*, 10−18.
(46) Mills, I. M. Vibration-Rotation Structure in Asymmetric- and Symmetric-Top Molecules. In *Molecular Spectroscopy: Modern Research*; Rao, K. N., Matthews, C. W., Eds.; Academic Press, 1972; Vol. *1*, pp 115−140.
(47) Becke, A. D. Density-functional exchange-energy approximation with correct asymptotic behavior. *Phys. Rev. A: At., Mol., Opt. Phys.* **1988**, *38*, 3098.
(48) Lee, C.; Yang, W.; Parr, R. G. Development of the Colle-Salvetti correlation-energy formula into a functional of the electron density. *Phys. Rev. B: Condens. Matter Mater. Phys.* **1988**, *37*, 785.
(49) Grimme, S.; Antony, J.; Ehrlich, S.; Krieg, H. A consistent and accurate ab initio parametrization of density functional dispersion correction (DFT-D) for the 94 elements H-Pu. *J. Chem. Phys.* **2010**, *132*, 154104.
(50) Grimme, S.; Ehrlich, S.; Goerigk, L. Effect of the damping function in dispersion corrected density functional theory. *J. Comput. Chem.* **2011**, *32*, 1456−1465.
(51) Frisch, M. J.; Trucks, G. W.; Schlegel, H. B.; Scuseria, G. E.; Robb, M. A.; Cheeseman, J. R.; Scalmani, G.; Barone, V.; Petersson, G. A.; Nakatsuji, H.; et al. *Gaussian16*, Revision C.01. Gaussian Inc.: Wallingford, CT, 2019; see http://gaussian.com.
(52) Mendolicchio, M.; Penocchio, E.; Licari, D.; Tasinato, N.; Barone, V. Development and implementation of advanced fitting methods for the calculation of accurate molecular structures. *J. Chem. Theory Comput.* **2017**, *13*, 3060−3075.
(53) Puzzarini, C.; Cazzoli, G. Equilibrium structure of methyl-cyanide. *J. Mol. Spectrosc.* **2006**, *240*, 260−264.
(54) Bizzocchi, L.; Prudenzano, D.; Rivilla, V. M.; Pietropolli-Charmet, A.; Giuliano, B. M.; Caselli, P.; Martín-Pintado, J.; Jiménez-Serra, I.; Martín, S.; Requena-Torres, M. A.; et al. Propargylimine in the laboratory and in space: millimetre-wave spectroscopy and its first detection in the ISM. *Astron. Astrophys.* **2020**, *640*, A98.
(55) Jaman, A. I.; Bhattacharya, R. Millimeter-wave rotational spectra of trans-acrolein (propenal)(CH_2CHCOH): a DC discharge product of allyl alcohol (CH_2CHCH_2OH) vapor and DFT calculation. *J. At. Mol. Phys.* **2012**, *2012*, 363247.
(56) Puzzarini, C.; Penocchio, E.; Biczysko, M.; Barone, V. Molecular Structure and Spectroscopic Signatures of Acrolein: Theory Meets Experiment. *J. Phys. Chem. A* **2014**, *118*, 6648−6656.
(57) Blom, C. E.; Bauder, A. Microwave spectrum, rotational constants and dipole moment of s-cis acrolein. *Chem. Phys. Lett.* **1982**, *88*, 55−58.
(58) Melli, A.; Potenti, S.; Melosso, M.; Herbers, S.; Spada, L.; Gualandi, A.; Lengsfeld, K. G.; Dore, L.; Buschmann, P.; Cozzi, P. G.; et al. A Journey from Thermally Tunable Synthesis to Spectroscopy of Phenylmethanimine in Gas Phase and Solution. *Chem.—Eur. J.* **2020**, *26*, 15016−15022.
(59) Bogey, M.; Demuynck, C.; Destombes, J. L.; Vallee, Y. Millimeter-Wave Spectrum of Formyl Cyanide, HCOCN: Centrifugal Distortion and Hyperfine Structure Analysis. *J. Mol. Spectrosc.* **1995**, *172*, 344−351.
(60) Caminati, W.; Vogelsanger, B.; Bauder, A. Rotational spectrum of styrene observed by microwave Fourier transform spectroscopy. *J. Mol. Spectrosc.* **1988**, *128*, 384−398.
(61) Thorwirth, S.; Lichau, H. The millimeter-wave spectrum and the dipole moment of vinylacetylene. *Astron. Astrophys.* **2003**, *398*, L11−L13.
(62) Brown, R. D.; Godfrey, P. D.; Winkler, D. A. Hyperfine interactions in the microwave spectrum of 2-propen-1-Imine (vinyl-imine). *Chem. Phys.* **1981**, *59*, 243−247.
(63) Müller, H. S. P.; Belloche, A.; Menten, K. M.; Comito, C.; Schilke, P. Rotational spectroscopy of isotopic vinyl cyanide, H2CCHCN, in the laboratory and in space. *J. Mol. Spectrosc.* **2008**, *251*, 319−325.
(64) Desyatnyk, O.; Pszczółkowski, L.; Thorwirth, S.; Krygowski, T. M.; Kisiel, Z. The rotational spectra, electric dipole moments and molecular structures of anisole and benzaldehyde. *Phys. Chem. Chem. Phys.* **2005**, *7*, 1708−1715.
(65) Jabri, A.; Kolesniková, L.; Alonso, E. R.; León, I.; Mata, S.; Alonso, J. L. A laboratory rotational study of the interstellar propynal. *J. Mol. Spectrosc.* **2020**, *372*, 111333.
(66) McGuire, B. A.; Burkhardt, A. M.; Kalenskii, S.; Shingledecker, C. N.; Remijan, A. J.; Herbst, E.; McCarthy, M. C. Detection of the

https://doi.org/10.1021/acs.jpca.1c07828
J. Phys. Chem. A 2021, 125, 9904−9916

aromatic molecule benzonitrile (c -C 6 H 5 CN) in the interstellar medium. *Science* **2018**, *359*, 202−205.
(67) Craig, N. C.; Groner, P.; McKean, D. C. Equilibrium Structures for Butadiene and Ethylene: Compelling Evidence for Π-Electron Delocalization in Butadiene. *J. Phys. Chem. A* **2006**, *110*, 7461−7469.
(68) Motiyenko, R. A.; Armieieva, I. A.; Margulès, L.; Alekseev, E. A.; Guillemin, J.-C. Rotational spectroscopy of malononitrile and its corresponding monoisocyanide isomer, isocyanoacetonitrile. *Astron. Astrophys.* **2019**, *623*, A162.
(69) McGuire, B. A.; Burkhardt, A. M.; Loomis, R. A.; Shingledecker, C. N.; Kelvin Lee, K. L.; Charnley, S. B.; Cordiner, M. A.; Herbst, E.; Kalenskii, S.; Momjian, E.; et al. Early science from GOTHAM: project overview, methods, and the detection of interstellar propargyl cyanide (HCCCH2CN) in TMC-1. *Astrophys. J. Lett.* **2020**, *900*, L10.
(70) Larsen, R. W.; Pawłowski, F.; Hegelund, F.; Jørgensen, P.; Gauss, J.; Nelander, B. The equilibrium structure of trans-glyoxal from experimental rotational constants and calculated vibration-rotation interaction constants. *Phys. Chem. Chem. Phys.* **2003**, *5*, 5031−5037.
(71) McNaughton, D.; Osman, O. I.; Kroto, H. W. The microwave spectrum and structure of Z-prop-2-ynylideneamine, HC-C-CH-NH. *J. Mol. Struct.* **1988**, *190*, 195−204.
(72) Raghavachari, K.; Trucks, G. W.; Pople, J. A.; Head-Gordon, M. A fifth-order perturbation comparison of electron correlation theories. *Chem. Phys. Lett.* **1989**, *157*, 479−483.
(73) Alessandrini, S.; Gauss, J.; Puzzarini, C. Accuracy of rotational parameters predicted by high-level quantum-chemical calculations: case study of sulfur-containing molecules of astrochemical interest. *J. Chem. Theory Comput.* **2018**, *14*, 5360−5371.
(74) Gardner, M. B.; Westbrook, B. R.; Fortenberry, R. C.; Lee, T. J. Highly-accurate quartic force fields for the prediction of anharmonic rotational constants and fundamental vibrational frequencies. *Spectrochim. Acta, Part A* **2021**, *248*, 119184.
(75) Buchanan, Z.; Lee, K. L. K.; Chitarra, O.; McCarthy, M. C.; Pirali, O.; Martin-Drumel, M.-A. A rotational and vibrational investigation of phenylpropiolonitrile (C6H5C3N). *J. Mol. Spectrosc.* **2021**, *377*, 111425.

https://doi.org/10.1021/acs.jpca.1c07828
J. Phys. Chem. A 2021, 125, 9904−9916